ChemPubSoc Europe

DOI: 10.1002/batt.201800102

BATTERIES & SUPERCAPS
Minireviews

Mg Cathode Materials and Electrolytes for Rechargeable Mg Batteries: A Review

Zheng Ma,[a] Douglas R. MacFarlane,[a] and Mega Kar*[a]

The development of energy storage devices has been motivated by the growing availability of sustainable energy sources, as well as the wider application of portable devices and a variety of electric vehicles including bicycles, scooters, cars and buses. Concerns regarding the safety of lithium batteries in certain applications, and limited lithium and cobalt resources required for conventional cathode materials, have driven researchers to develop alternatives that are safer and cheaper, thereby using more abundant metals such as sodium, magnesium, aluminium, and calcium. Among them, rechargeable magnesium batteries have drawn special interest, since Mg does not plate in a dendritic form, which opens up the possibility of the safe use of a simple metal anode. In this review, we summarize typical Mg electrolyte systems that are compatible with reversible Mg deposition and stripping, focusing on the active Mg complexes. To fabricate a rechargeable device, an appropriate cathode is necessary, which must also be abundant and compatible with the electrolytes to suitable cathode materials are also briefly discussed.

1. Introduction

Driven by the climate change and ocean acidification issues and the associated need to reduce dependence on fossil fuels, energy harvesting from renewable sources, such as solar, wind, tide and hydroelectric power, has expanded dramatically in recent years. Traditionally, electricity grids are directly used to distribute the electricity to households or factories; however, without energy storage devices, renewable electricity supply cannot be effectively regulated. This means that energy will be wasted, which is further aggravated by power losses through the massive grid transmission system. Most renewable energy harvesting techniques are intrinsically limited by the weather and geographic conditions, which additionally restrain their development and application.

Energy storage devices are thus of great importance to tackle these issues. When coupled with renewable energy harvesting techniques, energy storage devices enable the use of clean energy and offset the problem of unstable energy supply due to changes in weather, especially when the systems are installed in a distributed fashion.

Different energy storage devices have been explored, as shown in Figure 1.[1] Among them, secondary batteries such as Li-ion and Li-metal batteries, have gained extensive attention due to their high energy density.[2] Despite their attractively high energy density, Li-metal batteries suffer from several drawbacks, including growth of dendrites from uneven Li deposition at each charge-discharge cycle, causing short circuits. Li-ion batteries that use carbon-based anodes, prevent the formation of dendrites, however, instability of the typical cathode materials can still create a safety hazard. In addition, issues surrounding the potential scarcity of both lithium and also cobalt, an important component in many lithium cathode materials, are of concern in terms of very widespread use of large lithium-based devices. Thus, safer and more abundant alternative metals are required.

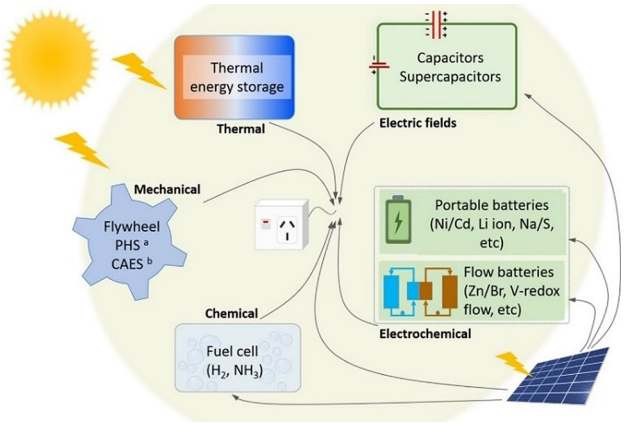

Figure 1. Classification of energy storage systems according to literature. [1] a PHS = pumped hydroelectric storage and b CAES = compressed air energy storage.

Mg has a redox potential of −2.37 V vs SHE. Being divalent it transfers 2 e- within a reduction and oxidation process, making up to some extent for its heavier atomic mass compared to Li. In an ideal metal-anode rechargeable battery, a bare Mg anode can offer a high volumetric charge capacity of 3.8 Ah cm^{-3} vs 2.0 Ah cm^{-3} for a Li anode. This translates to around 33 MJL^{-1} vs. 23 MJL^{-1} for Li. In gravimetric terms Mg delivers a theoretical energy density of around 19 MJkg^{-1}, compared to Li at 42 MJkg^{-1}; however, if one allows for the fact that both Li-ion and Li-metal batteries require the use of a

[a] Dr. Z. Ma, Prof. D. R. MacFarlane, Dr. M. Kar
School of Chemistry
Monash University
Clayton 3168, Victoria, Australia
E-mail: mega.kar@monash.edu

copper anode substrate foil, the practical energy density of lithium anodes is considerably lower than this.

Magnesium is also considerably more abundant (about 2.5% of the earth's crust) and available than Li (0.0017%). As a result, Mg is priced at around $2 per kg whereas $LiPF_6$, the most commonly used lithium salt in Li-ion batteries is around $43 per kg.

Another main advantage of Mg batteries is their potential for increased safety compared to lithium batteries. Mg deposits on the Mg anode are either a hemispherical or cauliflower-like morphology, both of which are unlikely to pierce separators and cause a short circuit. The lower reactivity of Mg (in comparison to Li) with air, rapidly forming a passivating coating of MgO, also contributes to a device with less likelihood of explosion.

2. Rechargeable Mg Batteries

Despite the advantages stated above, rechargeable Mg batteries (RMBs) are still at a research and development stage. One of the main challenges has been to find appropriate electrolytes which support efficient reversible Mg reduction and oxidation. In LIBs, the electrolyte generally decomposes at the electrode to form a solid electrolyte interface (SEI) layer, which is protective against further electrolyte breakdown, but still allows Li^+ ions to conduct. In RMBs, although a SEI layer may also be generated from the decomposition of the solvents on the Mg anode, this layer typically cannot readily conduct Mg^{2+} ions; instead, it is passivating. The issue here arises from the higher charge on the Mg ion which tends to cause it to bind strongly to many anionic and chelating species, hindering further movement. Figure 2 shows a schematic of more detail of SEI layer formation on a metal electrode in a non-aqueous solvent with impurities (such as H_2O) present in the electrolyte during the electrochemical processes; the role of water is particularly important in respect of Mg. Thus is is important to remove the water from the electrolyte and have a coordinating ligand (discussed below) to remove the native film and support reversible Mg electrochemistry.

In the present paper, the range of electrolytes for Mg batteries explored in the literature is reviewed, along with an electrolyte-related discussion of cathodes used in current RMB studies.

2.1 Organic Solvent Based Mg Electrolytes

To understand the complexities involved in electrolyte design it is important to understand the somewhat competing requirements of the electrolyte: Firstly, the purity of the Mg salts and solvents is critical for the anode, because impurities such as water can result in the formation of $Mg[OH]_2$ and MgO, forming passivating layers that will inhibit Mg deposition and dissolution (Figure 2). These passivating layers increase the magnitude of the reduction over-potential during charging (the energy needed to overcome the threshold created by the passivation layer on the electrolyte-electrode interface and/or to initiate nucleation and growth of the metal particles). Another critical factor is the Mg salt solubility. A high concentration of solvated Mg^{2+} ions is required for the avoidance of mass transport limitations. Solubility can be enhanced by the presence of species (either solvent molecules or additives) in the electrolytes that can coordinate to Mg^{2+}, to assist dissociation of Mg^{2+} ions, these complex ions must be redox active species as required for reversible Mg electrochemistry. Electrolyte systems must be thermally stable, sufficient to support stable battery operation at practical temperatures. Finally, in practical rechargeable batteries, electrolytes with high resistance to oxidation are required, to allow use of high voltage cathodes.

In regard to electrolyte solvent systems, aprotic polar solvents, such as propylene carbonate, ethylene carbonate and diethylene carbonate, which are widely used in LIBs, cannot be used in RMB electrolytes, as they are readily reduced on the Mg anode forming a passivating layer.[4] Most studies focus instead on the use of ether-functional solvents. These are typically compatible with Mg anodes and can stabilize Mg^{2+} ions via coordination through the electron-donating ether oxygens; however many of the examples are low boiling flammable materials that are not useful in practical RMBs.[5–7]

2.1.1 Mg–Al Transmetallation-Derived Mg Electrolytes

The first prototype RMB was reported by Aurbach's group, who used Grignard-derived Mg organohaloaluminate electrolytes, being mixtures of R_2Mg and R'_xAlCl_{3-x} (R or R′ = alkyl or aryl, x =

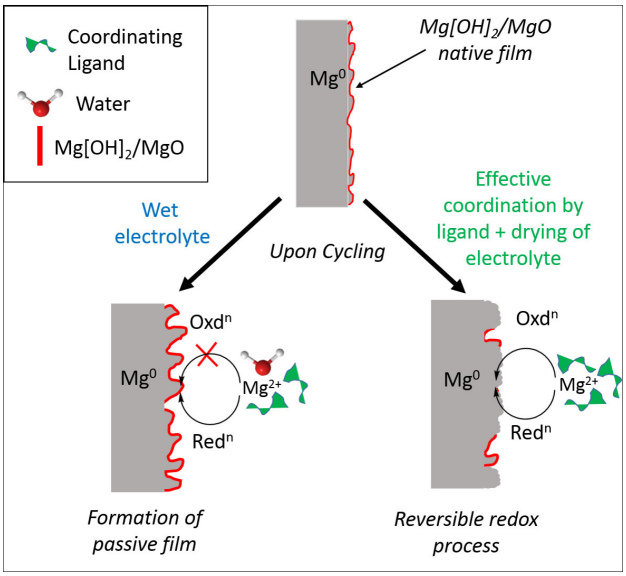

Figure 2. Upper: Formation of a native film on a Mg electrode upon exposure to trace amounts of moisture from surroundings prior to cycling. Bottom left: The presence of a wet electrolyte promotes the continued formation of a passive film on each cycle, hindering the re-oxidation of Mg. Water may dominate the coordination of Mg. Bottom right: In the presence of a coordinating ligand and complete removal of water cycling degrades the native film. This enables deposition of Mg on the bare metal electrode in each cycle, allowing subsequent oxidation.

0–3) in tetrahydrofuran (THF, b.p. = 66 °C)[7] along with a Chevrel phase Mo_3S_4 cathode material. The electrolyte supported good cycling at the anode between the dissolved species and Mg metal as depicted in Figure 3, while Mg^{2+} ion insertion and de-

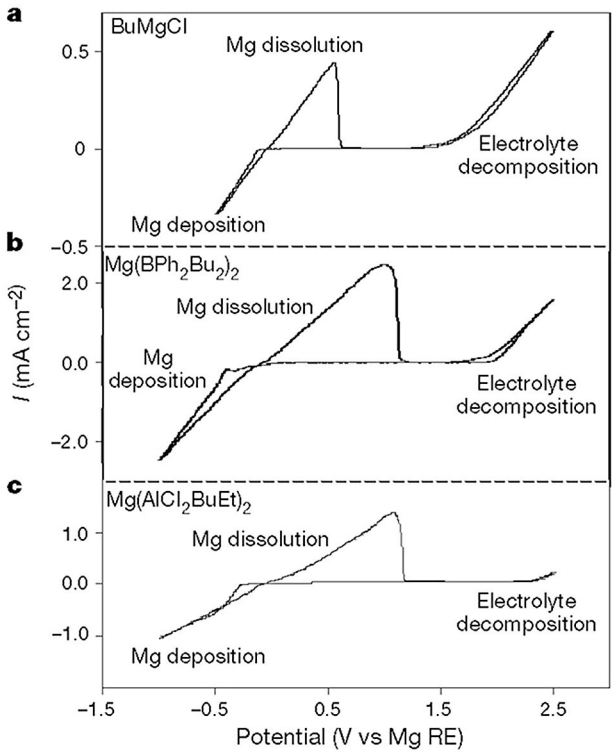

Figure 3. Typical cyclic voltammograms of Mg electrolytes in which magnesium can be deposited reversibly: **a**. BuMgCl/THF (2 M), **b**. $Mg(BPh_2Bu_2)_2$/THF (0.25 M) and **c** $Mg(AlCl_2BuEt)_2$/THF (0.25 M). Reprinted with permission from Ref. [7]. Copyright 2000 Macmillan Magazines Ltd.

insertion at two active sites in the channels of the Chevrel phase produced a discharge capacity of $>50\ mAh\,g^{-1}$ over 500 cycles; this will be further elucidated in cathode section. A series of studies on these organohaloaluminate/THF electrolytes investigated the active Mg species and the role of the Lewis acid R_xAlCl_{3-x} (x = 0,1 and R is a small alkyl group) in supporting reversible Mg electrochemistry.[3,7–15,16] A transmetallation reaction occurs between the R_2Mg base and R'_xAlCl_{3-x} acid and electrochemically active species such as $[MgCl]^+$ or $[Mg_2Cl_3]^+$ are generated during this transmetallation process (with the counter anions being $[R_nAlCl_{4-n}]^-$ (n = 1–4)). When the alkyl group R is substituted with phenyl groups to form the all phenyl complex (APC), a higher anodic stability was observed (3.2 V vs Mg),[17–18] which was attributed to a stronger bond between Al and the aromatic C.[17]

Similar to the organo-magnesium-chloroaluminate complexes discussed above, hexamethyldisilazide salts (HMDSMgCl or $HMSD_2Mg$) in the presence of ethers (such as THF and DME), also demonstrated compatibility as electrolytes with Mg for RMBs. The active species present in these electrolytes include cations such as $[MgCl]^+$ and $[Mg_2Cl_3]^+$, and anions $[HMDSAlCl_3]^-$, $[HMDS2AlCl_2]^-$, and $[HMDSMgCl_2]^-$.[19–24] Typically, $[MgCl]^+$ reacts with $MgCl_2$ forming $[Mg_2Cl_3]^+$, which is stabilized by coordinating with the ethereal oxygen atoms from the solvent, thus enabling Mg deposition and dissolution. A high cathodic stability up to 3.2 V vs Mg is also reported. The electrolytes additionally displayed compatibility with a sulfur cathode due to their non-nucleophilic properties.

When replacing the salts with a mixture of Mg hexafluoroisopropoxide ($Mg[HFIP]_2$) and Al hexafluoroisopropoxide ($Al[HFIP]_3$) in dimethoxyethane (DME), the electrolytes displayed higher ionic conductivity and also demonstrated reversible Mg deposition and dissolution.[25] Through a transmetallation reaction, weakly coordinating aluminate anions $[Al(HFIP)_4]^-$ formed, leading to highly dissociated active species and conductivity value $>6\ mS\,cm^{-1}$. Notably, the electrolytes showed high anodic stability, up to 3.5 V vs Mg. The high ionic conductivity could be attributed to the presence of highly ionized Mg^{2+} ions, which are stabilized by the ethereal oxygens in DME, while the anodic stability maybe a result of the strong Al–O bonding of the anion in the solution, owing to the high electronegativity of oxygen.[25]

Electrolytes containing inorganic salts, $MgCl_2$ and $AlCl_3$ (Magnesium-Aluminium-Chloro Complex, MACC) can also demonstrate reversible Mg cycling in ether solvents through a transmetallation interaction. The solubility of inorganic $MgCl_2$ salts in ether solvents can be enhanced by forming a $[Mg_2Cl_3]^+$ dimer in THF in the presence of $AlCl_3$.[26] The MACC electrolytes were found to exhibit a high anodic stability of up to 3.1 V vs Mg and a cyclic efficiency of ~98% at different stoichiometric ratios of $MgCl_2$ to $AlCl_3$.[27]

An electrochemical conditioning process was essential to achieve highly reversible Mg electrochemistry in MACC electrolytes.[28–32] Gewirth et al. reported that while Al^{3+}/Al reduction and partial oxidation was initially observed on a Pt working electrode, Mg^{2+}/Mg reduction and oxidation did not occur (Figure 4).[28] After approximately 30 cycles, an Al and Mg co-deposit was generated on the electrode with an improved cycling efficiency. After full conditioning, ~100 cycles, highly reversible Mg deposition occurred at a low reduction over-potential. The deposition of Al^{3+}/Al after the initial 100 cycles was not reported.

Chloride (Cl^-) anions play a significant role in the electrochemistry of MACC based electrolytes. Trace amounts of impurities, such as water and O_2 from Mg salts or solvents, are inevitably present within the electrolytes, and the resulting oxides (i.e. MgO) can lead to high over-potential and low reversibility of Mg (Figure 5a).[30] During the conditioning process, Al was reduced from the disassociated $[AlCl_4]^-$ onto the electrode, and thus Cl^- ion was released as a free anion into the solution; this Cl^- can adsorb onto the electrode surface and disrupt any passivating layer (through the process typically referred to as "pitting corrosion"[33]) (Figure 5b), to regain access to the active metallic substrate for active species to eventually exhibit reversible redox cycling.[30]

The concentration of components such as $AlCl_3$ is an important factor to consider in forming the active MACC electrolyte depicted in Figure 5b. The addition of excess $AlCl_3$ can cause the extraction of the free chloride ions from the Mg

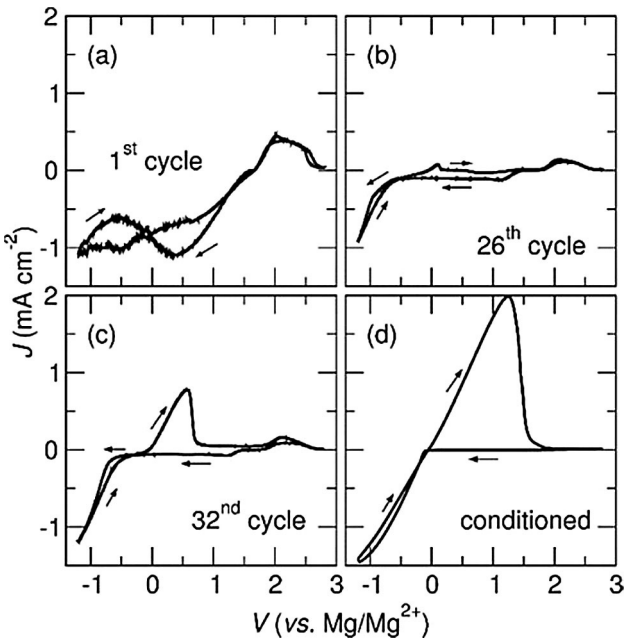

Figure 4. CV of MACC / THF before and after 100 cycles of "conditioning". Reprinted with permission from Ref. [30]. Copyright 2015 American Chemical Society.

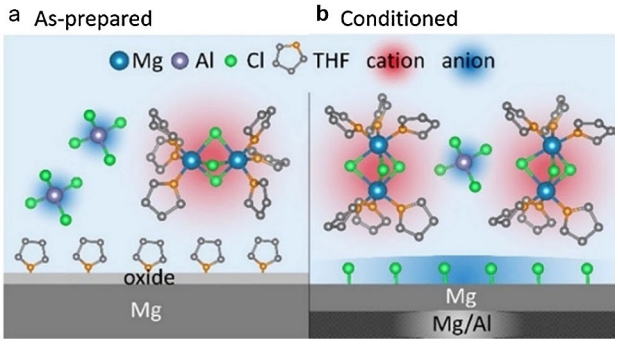

Figure 5. Scheme depicting speciation in the MACC electrolyte. a) as-prepared and b) conditioned. The conditioning process irreversibly electrodeposits Al resulting in a decrease in $[AlCl_4]^-$ concentration, an increase in $[Mg_2(\mu\text{-}Cl)_3{\cdot}6THF]^+$ concentration, and the formation of Cl^-. Cl^- decorates the electrode surface and promotes Mg electrodeposition. (Note stoichiometry is not preserved in this schematic). Reprinted with permission from Ref. [30]. Copyright (2016) American Chemical Society.

electrode surface, resulting in an increased over-potential and decreased efficiency. Alternatively, insufficient $AlCl_3$ can prevent dissolution of $MgCl_2$, inhibiting the formation of active electrolyte. In addition, the complex species occurs in equilibrium and thus over time can regenerate the starting components $AlCl_3$ and $MgCl_2$. Therefore, a second conditioning treatment is required to induce the re-arrangement of Mg–Cl–Al cluster and recover the active species.[28–31]

A major challenge in using MACC electrolytes for rechargeable batteries is also their high corrosiveness to the current collector and other metallic battery components. Thus, non-corrosive Mg electrolytes have been explored, as reviewed below.

2.1.2 Magnesium Borohydride Electrolytes

Mohtadi et al. showed that halide-free salts such as $Mg[BH_4]_2$ can partially dissociate in ethereal solvents such as THF and DME, supporting reversible Mg reduction and oxidation with efficiencies of 40% and 67%, respectively. In order to weaken the ion pair association of $Mg[BH_4]_2$ in solution, $LiBH_4$ was further added to the electrolyte, improving the coulombic efficiency to 94%.[34] The authors confirmed that no Li deposition was observed in the XRD, concluding that the coulombic efficiency was solely attributed to the cycling of Mg.

The weaker coordination of $[BH_4]^-$ anion to the cation enables the Mg salt to dissociate in ether solvents, which stabilize Mg^{2+} ions via coordination with oxygen; DME was found to be more effective than THF, because the ether oxygens in DME will coordinate more strongly, and increase the thermodynamic stability of the as-formed Mg^{2+} complex.[34,35] It was further found that, in comparison to DME, the addition of the extra oxygen atom in diglyme ($[CH_3–(–O–CH_2CH_2–)_3–]$ vs. DME $[CH_3–(–O–CH_2CH_2–)_2–]$) resulted in improved stripping kinetics of Mg^0.[35] The B–H hydrogen bridge formation as well as the higher oxygen-donating number in diglyme seems to improve the stability of the Mg complex and be beneficial to the reversible plating and stripping.

2.1.3 Magnesium Carborane Electrolytes

Since $[BH_4]^-$ is a strong reducing reagent, the low anodic stability of $[BH_4]^-$ (1.7 V vs Mg) is the main limitation of these electrolytes[34] in supporting battery operation in the target region of 3 to 4 V. Thereafter, Mohtadi et al. synthesised boron-based anions with increased oxidative stability.[36–38] Initial efforts revealed that *closo*-borane $Mg[B_{12}H_{12}]_2$, which has a high anodic stability above 4 V vs Mg, is not soluble in ethers. In contrast, it was found that electrolytes containing carboranyl magnesium halides $[Mg(C_2B_{10}H_{11})Cl]^-$ and $[Mg_2Cl_3]^+$ in THF can exhibit electrochemical cycling of Mg with a coulombic efficiency of 98%. Although not as high as $Mg[B_{12}H_{12}]_2$, the carboranyl magnesium halides can still demonstrate an oxidative stability up to 3.2 V vs Mg on a Pt substrate.[36] In an effort to move away from corrosive chloride-based species, an icosahedral Mg salt with *closo*-monocarborane (MMC) $[CB_{11}H_{12}]^-$ anion (which is more lipophilic than $[B_{12}H_{12}]^{2-}$ due to the charge reduction) was synthesised and electrochemically tested in glyme-based solvents.[37–38] It was elucidated that, since the $[CB_{11}H_{12}]^-$ anion is a weak nucleophile, especially because the anionic charge is delocalized over the cage, the coordinating Mg–C bond was weak enough to be dissociated in low polarity solvents. The electrolyte based on MMC/tetraglyme resulted in a coulombic efficiency $>94\%$, while the oxidative stability was found to be as high as 3.8 V vs. Mg (Figure 6). Coin cells containing Mg anodes and 0.75 M MMC in tetraglyme were tested with various cathodes. Stable charge-discharge capacities $>80\ mAh\,g^{-1}$ were obtained in the presence of Chevrel phase Mo_6S_8 cathodes while capacities $>90\ mAh\,g^{-1}$ were obtained with α-MnO_2 cathodes for 10 cycles in each case.

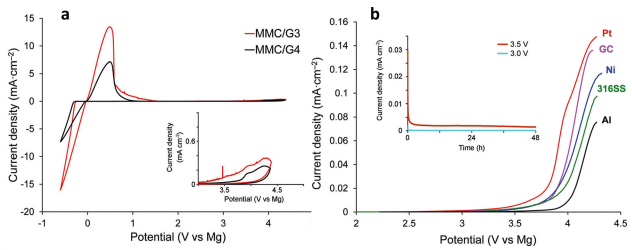

Figure 6. a) CV of 0.75 M MMC in triglyme (G3) (red) and tetraglyme (G4) (black) on Pt working electrode. (Cycle 1; inset: CV in the region between 3.0–5.0 V). b) LSV of 0.75 M MMC in tetraglyme (G4) electrolyte on various (inset: chronoamperometry of 0.75 M MMC/G4 electrolyte on 316SS disk electrodes (area: 1.33 cm^2) at 3.0 V (light blue) and 3.5 V (brown) vs. Mg.) (Scan rate: 5 mVs^{-1}). Reprinted with permission from Ref. [37]. Copyright 2015 WILEY-VCHVerlag GmbH & Co. KGaA, Weinheim.

2.1.4 Magnesium Organoborate-Based Electrolytes

Electrolytes of Mg organoborate salts containing borate-centred anions were recently reported to support reversible Mg plating and stripping.[39–41] Cui's group reported functional electrolytes comprising of bulky organoborate anions with fully fluorine-substituted propoxide chains.[41] With the addition of tris(2H-hexafluoroisopropyl) borate (THFPB), MgF_2 salt was partially dissolved in DME, to generate the anion and cationic species $[FTHB]^-$ and $[Mg(DME)_n]^{2+}$ respectively (Figure 7a and 7b). The formation of the $[FTHB]^-$ anion is attributed to the affinity between the boron centre of THFPB and the F^- anion which is strong enough to dissociate MgF_2. Additionally, the coordination between the metal ion and the ether oxygen atoms in DME, enables the formation of the stable $[Mg(DME)_n]^{2+}$ cation. Interestingly, upon electrochemical cycling of this magnesium organoborate electrolyte, ($[TrHB]^-$) (also known as $[B(HFIP)_4]^-$) anions were generated (Figure 7c) as confirmed via NMR and Raman spectra. Furthermore, the cyclic efficiency of Mg from this newly formed electrolyte improved with cycling and an anodic stability of 3.5 V vs Mg (on stainless steel) was reported. The non-nucleophilic nature of organoborate anions also make these electrolytes compatible with sulfur cathodes, and thus potentially suitable for high energy density devices. Recently the same group also reported a novel magnesium electrolyte comprising of $[B(HFIP)_4]^-$ anion couple with a solvated $[Mg_4Cl_6(DME)_6]^{2+}$ cation, demonstrating an anodic stability of 3.3 V vs. Mg and a coulombic efficiency of

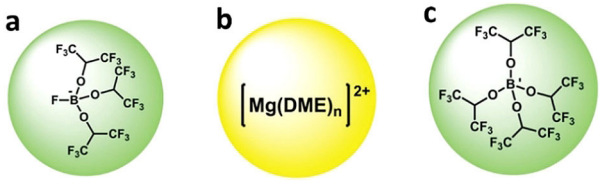

Figure 7. Structures of the proposed active cation and anion in the tetra (hexafluoroisopropyl)borate Mg electrolytes. a) the incipient anion species $[FTHB]^-$ in fresh electrolyte; b) the active cation species in electrolyte; c) the anion species $[TrHB]^-$ in cycled electrolytes. Reprinted with permission from Ref. [41]. Copyright 2017 WILEY-VCHVerlag GmbH & Co. KGaA, Weinheim.

98% over 300 cycles. The electrolyte was also shown to be compatible with sulfur cathodes, exhibiting a discharge capacity >1000 $mAhg^{-1}$ over 100 cycles. However, the addition of chloride ions in the electrolyte can cause corrosion to current collectors such as aluminium in conventional batteries. The synthesis of $Mg[B(TrHB)_4]_2$ via MgO was also reported by the same group.[40]

A more effective method was reported by Zhao-Karger et. al. to involve synthesis of the magnesium borate salt $Mg[B(HFIP)_4]_2$ from $Na[B(HFIP)_4]$ and $MgBr_2$ in DME, forming highly conductive electrolytes (6.8 $mS\,cm^{-1}$).[39] These electrolytes showed high anodic stability, especially on a stainless steel (SS) electrode (up to 4.3 V vs Mg). For the anion, since each boron centre is bonded to four oxygens from the fluorinated propoxide, electrons are well-delocalized from the electron-rich B–O bonds through the adjacent electron-withdrawing fluorinated group. Thus, the anions exhibit weak electrostatic interactions with Mg^{2+} cations, enabling the metal ion to be readily dissociated and coordinate to the ether oxygens of DME. In comparison to pure DME, the formation of such solvates (i.e., $[Mg(DME)_n][B(Hfip)_4]$) additionally increase their thermal stability. Recently the same group thoroughly investigated the use of borate salt $Mg[B(HFIP)_4]_2$ in a full Mg/S cell[42] (See Table 3).

2.1.5 $Mg[NTf_2]_2$ Electrolytes

Owing to the weak ion-pairing interaction between large anions and Mg^{2+} cations, Mg di[bis(trifluoromethylsulfonyl) imide] ($Mg[NTf_2]_2$, also known as $Mg[TFSI]_2$) salts have the potential to be dissolved in high concentrations in aprotic polar organic solvents producing highly conductive electrolytes.[43,44] Also, the charge-delocalized framework makes this conjugated $[NTf_2]^-$ anion highly resistant to positive potential polarization,[45] and thus high anodic stability can be expected in such electrolytes. There have been a number of studies using $Mg[NTf_2]_2$ in different solvents for reversible Mg electrochemistry, particularly in polyether(s).[43,46–61] Electrolytes using 0.5 M $Mg[NTf_2]_2$ in a glyme/diglyme mixture showed a high conductivity of 5.2 $mS\,cm^{-1}$, and the anodic stability on stainless steel (SS) substrate was up to 4.2 V vs Mg.[46]

Glymes with higher oligomer degree exhibit stronger ability to solvate $Mg[NTf_2]_2$.[43,51] For example, a higher solubility of Mg has been reported in tetraglyme (G4) than in diglyme (G2).[43] On the other hand, the viscosity of the G4 electrolytes will be greater, resulting in lower conductivity and higher overpotential for Mg deposition. Watanabe's work revealed that, in $Mg[NTf_2]_2$/tetraglyme electrolytes, a solvate type IL formed, containing $[Mg(G4)]^{2+}$ cations (typically a Mg^{2+} ion was chelated by four oxygen atoms of one G4) and $[NTf_2]^-$ anions.[58]

Some studies have revealed that, in Mg electrolytes containing $[NTf_2]^-$ anions, the decomposition of $[NTf_2]^-$ can occur during the Mg reduction process.[62] The process was described in the following order: acceptance of the first electron causes formation of a $Mg^+[NTf_2]^-$ intermediate, breaking of the S–C bond of $[NTf_2]^-$, and formation of $Mg[CF_3]_2$ as an

insoluble passivation layer on the metallic electrode.[51] Reductive decomposition via scission of the S–C bond has been discussed also in Li[NTf_2] based electrolytes and ionic liquids.[63]

In the presence of water, Mg[NTf_2]$_2$ salts can easily crystallize as the hexahydrate Mg[NTf_2]$_2$·6H_2O. It was shown that, in a Mg[NTf_2]$_2$/G4 electrolyte, even with a vigorous drying treatment of the Mg[NTf_2]$_2$ salt, the water content *increased* after Mg cycling, which indicates that water molecules entrained as part of a $[Mg(H_2O)_6]^{2+}$ hydrate ion are released after the Mg^{2+} ions were reduced.[58] The free H_2O molecules readily react with Mg species forming inactive Mg[OH]$_2$ and MgO. Aurbach's studies showed that adding $MgCl_2$ to Mg[NTf_2]$_2$/DME electrolytes enables nearly 99% reversible Mg reduction and oxidation performance.[53] When there are no Cl^- species present in Mg[NTf_2]$_2$ based electrolytes, dehydrating reagents are needed to inhibit the formation of a passivating layer. It has been reported that reversible Mg electrochemistry can take place after removing the H_2O by molecular sieves or by reaction with trace amounts of Bu_2Mg or Mg[BH_4]$_2$.[53,60]

2.1.6 Magnesium Electrolytes with Non-Ether Solvents

Acetonitrile (AN), which can act as an electron-donating ligand, was also used as a solvent with Mg organohaloaluminate salts for reversible Mg electrochemistry. Studies on Mg electrolytes in AN have shown contradictory results. One study claimed that, in Mg[ClO_4]$_2$/AN electrolytes, a thick passivation layer formed on the electrode with Mg plating at high overpotential.[64] However, another study revealed the decomposition of acetonitrile at a cathodic potential, mimicking the reduction current of Mg deposition, due to the reduction potential of AN (−2.5 V vs SHE) being close to that of Mg^{2+}/Mg (−2.37 V vs SHE).[65] The electrolytes only demonstrated the feasibility of reversible Mg intercalation into the cathode materials used. Overall, use of acetonitrile as a solvent for Mg electrolytes is still an open question.

2.2 Ionic Liquid Based Mg Electrolytes

Room temperature ionic liquids (RTILs) generally have good conductivity and fluidity.[66] The ion-pair interactions in the ILs are weakened by the steric hindrance of the bulky organic cations as well as the delocalized charge density of the anions. Most aprotic ionic liquids have high thermal stability (i.e., Td $\geq$ 300 °C), negligible vapor pressure and low flammability. By changing the functional groups of the cations and/or anions, ILs can be designed with specific physical and electrochemical properties, which have been widely used in different electrolyte systems.[67–73] Overall, using ILs as solvents or co-solvents in electrolytes for storage devices may increase their thermal stability, extend their electrochemical operating window and improve their conductivity.

2.2.1 Neat Ionic Liquid Based Mg Electrolytes

The first study of ILs as solvents for Mg electrolytes investigated 1-Butyl-3-methylimidazolium tetrafluoroborate ([C4mim][BF_4]) and Mg[NTf_2]$_2$.[74] Although reversible electrochemistry was initially reported in these electrolytes, and deposits were obtained from galvanostatic deposition, the onset reduction potential was more negative than −1.0 V vs Mg, and the peaks observed in the cyclic voltammogram cannot be assigned to typical Mg reduction and oxidation behaviour. The lack of evidence (such as XRD characterization) to confirm Mg deposition casts doubt on the reversibility of these electrolytes. Subsequent studies employing the same electrolytes displayed irreversible Mg electrochemistry.[47,75,76] The strong interactions between Mg^{2+}, and $[BF_4]^-$ or $[NTf_2]^-$ were speculated to be responsible for the high over-potential that can ultimately drive the decomposition of the electrolyte ions, forming passivating layers on the electrode.[47,75] According to our study,[60] H_2O impurities could also be responsible for the irreversibility of Mg in $[NTf_2]^-$-based electrolytes.

To date, the electrochemical reversibility of Mg has been studied in two different families of IL based electrolytes: (1) Imidazolium based ILs such as 1-Ethyl-3-methylimidazolium chloride ([C_2mim]Cl) with MACC[77] and [C_2mim][AlI_4] with MgI_2,[78] and (2) ether-based IL electrolytes containing Mg[BH_4]$_2$.[73,79] In type (1) electrolytes, similar to the above-mentioned MACC electrolytes, the active species for reversible Mg reduction and oxidation are generated from the transmetallation of the Lewis acid AlX_3 (X=Cl, I) and the Lewis base MgX_2 (X=Cl, I) in the solution, which also produces free halide ions. In a very different process, the ether-based IL electrolytes (2) contain Mg^{2+} ions dissociated from Mg[BH_4]$_2$ in the ILs. Figure 8 shows typical CVs in IL-based Mg electrolytes, along

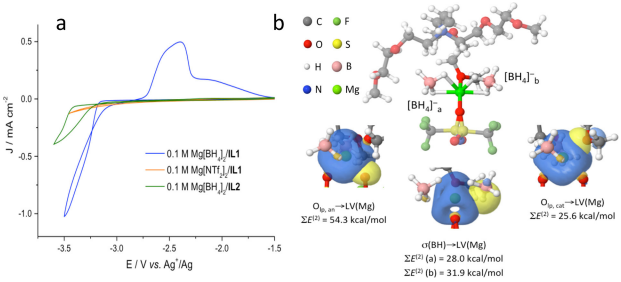

Figure 8. a) CVs demonstrating reduction and oxidation of Mg from 0.1 M Mg[BH_4]$_2$/IL1 (blue), 0.1 M Mg[NTf_2]$_2$/IL1 (orange), and 0.1 M Mg[BH_4]$_2$/IL2 (green). IL1: tri-alkoxy ammonium bis(trifluoromethanesulfonyl)imide [N2(20201)(20201)(20201)][NTf_2], IL2: tri-alkoxy ammonium bis(fluorosulfonyl) imide [N2(20201)(20201)(20201)][FSI]. b) Mg[BH_4]$_2$/IL1 electrolyte showing main NBO contributions around the Mg2+ ion. Reprinted from Ref. [73] with permission of The Royal Society of Chemistry, copyright (2016).

with the proposed coordination structure of the Mg^{2+} complex;[73,79] these Mg^{2+} ions can be coordinated by both $[NTf_2]^-$ anion and the IL cation, which contains an electron-donating oxygen. It was deduced that the cationic polyether oxygen coordination to Mg^{2+} can replace that of $[NTf_2]^-$ and partially

replace $[BH_4]^-$, to enable reversible Mg reduction and oxidation.[73]

2.2.2 Organic Solvent/Ionic Liquid Mixture Based Mg Electrolytes

However, in most cases, ILs are used as co-solvents in Mg electrolytes along with THF or a glyme solvent. Adding ILs can often enhance certain electrochemical and physical properties of the electrolytes. Thus far, ILs such a butyl-1 methylpyrrolidinium trifluoromethanesulfonate [C4mpyr][OTf],[75] diethylmethyl(2-methoxyethyl)ammonium bis(trifluoromethylsulfonyl)imide [DEME][NTf_2],[4] and others, when mixed with ethereal solvents, have been shown to support reversible Mg reduction and oxidation with various Mg salts, including Grignard salts, Mg organohaloaluminates, MACC, $Mg[BH_4]_2$, and $Mg[NTf_2]_2$. In comparison to an electrolyte composed of a Mg salt in an organic solvent, the conductivity is significantly enhanced by the addition of the IL. For example, conductivities of 0.33 mS cm^{-1} and 7.44 mS cm^{-1} were measured for EtMgBr/THF electrolytes before and after addition of [DEME][NTf_2].[4] Notably, the conductivity of these mixed electrolytes was also higher than that of the neat IL, However, in another case, the conductivity of the electrolyte decreased due to elevation of viscosity.[20] Generally, it can be concluded that, compared to neat organic solvent based Mg electrolytes, the introduction of ILs at a low content can improve the ionic conductivity of the electrolytes and enhance the active-ion transfer in the electrolytes.[24,80] Our recent work also showed that the thermal stability of Mg electrolytes can be enhanced when the organic solvent was partially replaced with IL.[81] However, as the percentage of IL increases the ionic interactions between the ions in the electrolytes typically become an obstacle to ion transfer.[56] As a result, the viscosity of the electrolyte increases and the ionic conductivity decreases, leading to increased overpotentials and decreased current densities in reduction and oxidation cycling.[82]

Other than using ILs directly as solvents or co-solvents for electrolytes, studies by Watanabe's group designed solvated ILs containing Mg^{2+} ions, which were prepared by dissolving $Mg[NTf_2]_2$[58] in tetraglyme (G4) at a certain stoichiometries. Typically, these solvated ILs contained $[Mg(G4)]^{2+}$ cations – Mg^{2+} coordinated by a four-oxygen-atom cage from one G4 molecule – and $[NTf_2]^-$ anions. The advantage of these electrolytes is the combination of a high degree of dissociation of Mg^{2+} and high fluidity of the solution. These electrolytes also show relatively high thermal stability due to the absence of any free glymes.[58] The electrochemical reversibility of Mg reduction from 0.5 M $Mg[NTf_2]_2$ in tetraglyme has been demonstrated, as discussed above (See Section on $Mg[NTf_2]_2$ electrolytes).

2.3 Metallic Electrode Interface in Mg Electrolytes

In contrast to the conductive Solid Electrolyte Interface (SEI) layer in LIBs, the SEI formed on the electrode in Mg electrolytes due to the decomposition of solvents and the presence of impurities such as H_2O, is likely composed principally of MgO formed as a passivation layer (as illustrated in Figure 2) and inhibiting conduction of Mg^{2+} ions.[3] As a result, Mg reduction normally requires a high over-potential to overcome the energy barrier,[55] which induces a distinct morphology in the Mg deposit. As illustrated in Figure 9,[83] during the reduction

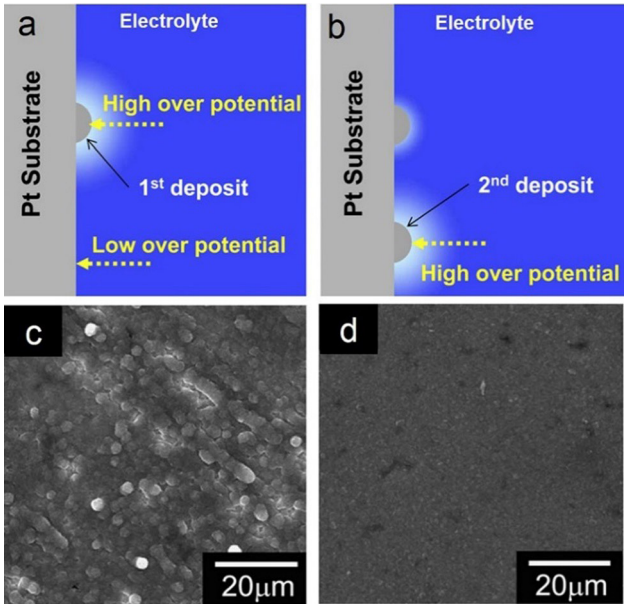

Figure 9. Sacnning image of Mg deposition showing: a) the first deposits, b) further deposit (color of the electrolyte represents the Mg^{2+} concentration). SEM images of electrodeposited magnesium from a Mg electrolyte of 2 M EtMgCl/DimetylAlCl/THF, 0.37 ml of dimethylaluminum chloride at a current density of c) 0.5 mA cm^{-2} and d) 2 mA cm^{-2}. Reproduced with permission from Ref. [83], Copyright 2010 Elsevier.

process, initially a Mg deposit nucleates on the electrode (1st deposit in Figure 9a) at a certain potential and becomes passivated by the SEI layer. Compared to the Mg nucleation and growth on a different area of the naked Pt substrate (2nd deposit in Figure 9b), higher over potential is needed to deposit more Mg on the 1st deposit. Eventually, the distribution of the reduced Mg^0 particles covers all of the Pt substrate, preventing dendrite formation and producing a cauliflower type morphology.[32,55,83,84]

Mg salts and other electrolyte species can influence the overpotential for Mg reduction and oxidation, especially in the presence of trace H_2O in the electrolytes. For instance, while Grignard salts, organohaloaluminate Mg salts and $Mg[BH_4]_2$ are highly reactive with water tending to inhibit its role in the Mg electrochemistry, less reactive electrolytes, such as those containing $MgCl_2$ or $Mg[NTf_2]_2$ are easily hydrated and difficult to dry thoroughly by pre-heating. Studies show that with pretreatments to these electrolytes via either voltammetric cycling for MACC electrolytes,[28–31] or adding an H_2O scavenger to the electrolytes,[53,58,60] highly reversible Mg electrochemistry can be obtained. Mg powder was also found to be effective to remove impurities from the electrolytes.[85]

As discussed above, in MACC electrolytes, during cycling conditioning, an amount of free Cl^- generated during the pre-conditioning can adsorb onto the electrode surface and induce pitting corrosion, which will also be corrosive to the current collector in the same way. If the water content can be controlled to be less than 10 ppm, the initial cycling conditioning treatment may not be necessary.[32]

Various modification methods to Mg anodes have been developed to diminish the influence of the passivation layer at the Mg electrode interface.[86–88] It has been demonstrated that after surface treatment with $Ti[NTf_2]_2Cl_2$, the Mg anode was compatible with $Mg[TFSI]_2$/DME/G2 based electrolytes. It is believed that $Ti[NTf_2]_2Cl_2$ can chemically etch the insulating MgO species, thus activating the Mg surface to enable reversible Mg electrochemistry.[86] Another surface modification method showed that by engineering a conductive layer on the Mg anode, a Mg cell can be constructed with a V_2O_5 cathode and $Mg[NTf_2]_2$ electrolyte, even in the presence of H_2O. This work has addressed the H_2O passivating issue while maintaining the charge shielding effect of H_2O with respect to Mg^{2+} that is significant on the cathode.[87] In other work, Chen et al. synthesized Mg nanoparticles and used them as the anode material to achieve reversible Mg electrochemistry. It was hypothesized that, compared to a bulk Mg electrode, the surface passivation film formed on the electrode is much thinner due to the high surface area of the Mg nanoparticles.[88] However, the Mg–Al transmetallation-derived type electrolytes used in this study still suffer from the drawback of being highly corrosive.

The over potential for Mg reduction influenced by the nature of the dissolved Mg salt. In a fluid electrolyte, when a high concentration of active Mg^{2+} species present, facile kinetics of the reduction process can be expected. According the studies by Matsui[83] and Ling,[89] when a high deposition rate is then applied, low dimension growth of Mg^0 produces a more planar morphology due to high nucleation rates (Figure 9a and 9d).[83,89–91]

2.4 Cathode Materials for Mg Batteries

Although different Mg electrolytes systems have been developed, including some producing high reduction-oxidation cycling efficiency, Mg rechargeable batteries are still far from a commercial reality. This is partly due to the lack of options for cathode materials which can be operated at high positive voltages and support a usefully high energy density. The conventional transition-metal oxide cathodes for Li batteries are not effective for Mg^{2+} ion insertion due to the slow diffusion of the divalent Mg^{2+} cations; their high charge density leads to strong electrostatic interactions with the host lattice.[92] Cathode materials for RMB have been reviewed previously.[93–95] Herein, a brief overview of cathode materials from the electrolyte viewpoint will be provided.

2.4.1 Molybdenum Chalcogenides

Chevrel phase Mo_6S_8 (theoretical capacity of 122 mAh g^{-1}) was the first cathode material to show compatibility with a wide range of Mg electrolytes.[7] This material has a three-dimensional open structure, made up of Mo_6S_8 blocks, each of which contains a Mo_6 octahedral cluster inside a S_8 cube. Typically, Mg^{2+} cations can easily insert and de-localize into the active sites between the channels.[7,94,95] The variable valence of the Mo_6 cluster can easily compensate the charge-unbalance caused by the introduction of divalent ions during insertion to maintain electroneutrality.[94,95] Since electronic charges can re-distribute readily on each element (Mo or S) of the cluster, a weak interaction is expected with the guest cation, allowing Mg^{2+} ions to diffuse in a multi-directional pathway and easily intercalate in the host material. The material can exchange up to four electrons.[7]

The first Mg^{2+} ion insertion takes place at 1.2 V vs Mg (Figure 10), (Site A) and the second Mg^{2+} ion insertion takes place at 1.0 V vs Mg (Site B), since there is a phase transition after the first Mg^{2+} intercalation which alters the insertion energy.

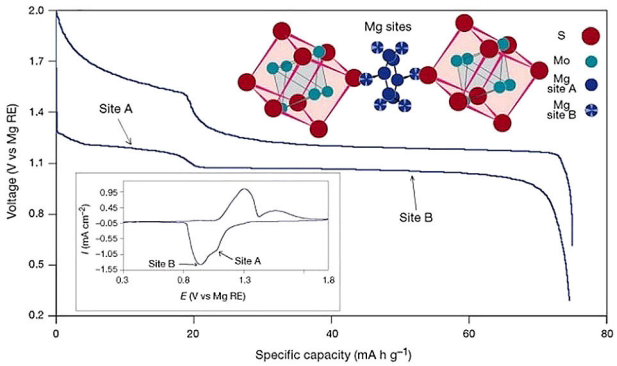

Figure 10. Crystal structure of Chevrel phase Mo_6S_8 and its charge-discharge performance in $EtMgCl/EtAlCl_3$/THF electrolyte. Reprinted with permission from Ref. [7]. Copyright 2000 Macmillan Magazines Ltd.

However, the application of this material for practical Mg rechargeable batteries is limited by its low theoretical capacity (122 mAh g^{-1}) and low output voltage ($<$1.5 V). Despite this, because it is able to maintain a stable structure, Mo_6S_8 has become the standard cathode for use in laboratory studies of Mg electrolytes.[44]

The cycling performance of typical electrolyte systems with this cathode is summarized in Table 1.

Beyond the Chevrel phase cluster cathode, other types of molybdenum chalcogenide materials are also studied as cathodes for RMB. As an example, nanostructured MoS_2 with a higher theoretical energy capacity of 223 mAh g^{-1} was also studied, but the performance was not as good as that of Chevrel phase Mo_6S_8 in terms of the cyclability.[88] Other cathode materials of this kind have been described.[93–99]

Table 1. Summary of performance of Chevrel phase Mo_6S_8 cathode with Mg anode and different Mg electrolytes in laboratory magnesium batteries.

Electrolytes	Output voltage [V]	Initial capacity [mAh g^{-1}]	Final capacity [mAh g^{-1}]	Cycles	Coulombic efficiency	Ref. No
0.25 M $Mg[AlCl_2BuEt]_2$/THF	1.2	80	55	580	…	[7]
0.25 M $Mg[NTf_2]_2$/0.5 M $MgCl_2$/DME	0.85	80	…	10	…	[53]
0.5 M $Mg[BH_4]_2$/G4	0.9	65.9	…	…	…	[100]
1.2 M $[(CF_3)_2(CH_3)]$COMgCl/0.2 M $AlCl_3$/THF	1.1	104	97	5	…	[101]
0.5 M $Mg[NTf_2]_2$/0.15 M $Mg[B(OPh)_3]_2$/0.1 M $MgCl_2$/G2	1.0	80	94	40	96%	[59]
0.25 M $Mg[HFIP]_2$/0.5 M $AlCl_3$/DME	1.0	112	56	50	…	[102]
0.8 M $MgCl_2$/DPSO/THF	1.0	125	72	300	98%	[103]
0.625 M $Mg[HMDS]_2$-$MgCl_2$/THF/DEMETFSI	1.05	62	47	40	…	[24]
0.8 M $Mg[NTf_2]_2$/DME/G2	0.9	87	30	70	…	[86]
0.05 M MgO/0.2 M THFPB/DME	1.1	83	46	400	~100%	[40]

2.4.2 Transition-Metal Compounds

MoO_3,[14] V_2O_5,[56,104–105] MnO_2,[106–110] and TiO_2[111–113] have been prepared with different structures. Most of these transition metal compounds are nanosized, to provide a high surface area with more active sites for cation intercalation as well as short ion-transport paths to facilitate cation diffusion.[44,114] However, with their high charge density, Mg^{2+} ions are restricted by their strong electrostatic interaction with the electron-rich oxygen centres, and become trapped in the solid-state lattice.[94–95,97,99,115] The cyclability and cycling efficiency of these cathode materials are typically not high, due to the highly irreversible Mg intercalation behaviour. A small amount of H_2O is then generally used in the cathode reaction to shield the divalent Mg^{2+} charge by hydration, facilitating the insertion and removal of Mg^{2+} ions into/from the oxide cathode to obtain improved cyclability.[94,116,117] However, as discussed in the previous section, H_2O is not compatible with the anode, and will cause the formation of a passivation layer. Thus, although they provide a higher operating voltage, the use of these transition-metal oxides is still limited.

Since Mg^{2+} ions do not intercalate well into most available transition-metal oxide cathode materials, "dual-salt" systems employing Li salts or Na salts as the charge carriers for the cathode reaction in rechargeable Mg batteries have been studied. In the dual-salt electrolyte system, the electrolyte also contains a high concentration of monovalent Li^+ ions or Na^+ ions. Ideally, metallic Mg acts as the anode process (well above Li potential), while smaller Li^+ ions or Na^+ ions can intercalate or de-intercalate into traditional cathode materials. Figure 11 displays a charge-discharge circuit of a working RMB using Mg dual-salt electrolytes, and some possible cathode materials for typical Mg dual-salt systems.

Studies on transition-metal oxide cathodes with various Mg dual-salt electrolytes (containing both Mg and Li/Na salts) have thus been reported.[111,113,118–126] Compared to Mg salts, the monovalent property of Li and Na salts means that they have weaker electrostatic interactions and lower co-ordination numbers, making them more soluble in the solvents. For instance,[119] $LiNTf_2$ showed a higher solubility in diglyme than that of $Mg[NTf_2]_2$ Highly reversible charge-discharge behaviour is observed in some of these Mg hybrid systems, with reasonable output voltage and energy capacity. Since dendrite-forming species are present in the electrolytes, the cut-off limit for charging should be carefully limited to avoid plating lithium or sodium metal.

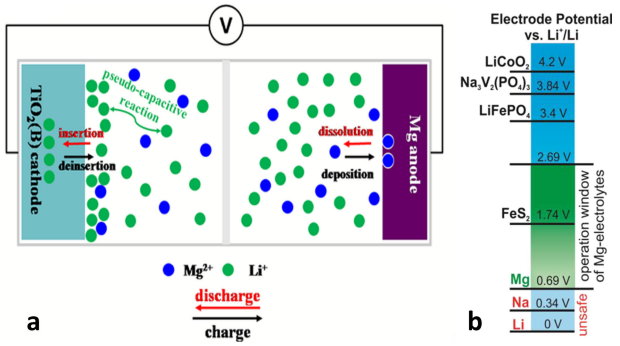

Figure 11. Schematic of a) Mg rechargeable battery using Mg/Li hybrid electrolytes. Reprinted with permission from Ref. [111]. Copyright 2016 American Chemical Society. b) Possible cathodes for Mg/Li or Mg/Na hybrid electrolytes. Reprinted with permission from Ref. [120]. Copyright 2016 American Chemical Society.

Detailed discussion of Mg dual-salt electrolytes containing Li salts can be found in a recent review.[122] Some of the latest studies using different cathodes in Mg dual-salt electrolytes are collated, along with their charge-discharge performance, in Table 2.

2.4.3 Conversion Cathodes

Sulfur, S_8, can serve as a conversion-type cathode material for rechargeable metal batteries, and has a high theoretical energy capacity of 1671 mAh g^{-1}. Mg/S batteries have also been studied recently.[19,20,39–41,127,128] The initial active cathode material is S_8, and a non-nucleophilic environment is needed to avoid reaction with the cathode. Most effective Mg electrolytes, such as Grignard-based systems; or Mg organohaloaluminate electrolytes, contain nucleophilic groups such as ethyl, butyl, or phenyl, which are reactive with electrophilic sulfur. HDMSMgCl/$AlCl_3$/THF solution was explored as the first non-nucleophilic electrolyte, and was compatible with a sulfur cathode for Mg/S batteries. An initial discharge capacity of 1200 mAh g^{-1} was found, but the cyclability was poor, and the capacity decayed drastically.[19]

The cathodic reactions in an Mg/S battery during discharge are:[22]

Table 2. Summary of performance of different transition-metal based cathodes with Mg anodes and various Mg hybrid electrolytes in laboratory magnesium batteries. (*OMBB = $[Mg_4Cl_6(DME)_6]^{2+}$ $[BHFP_4]^-$).

Cathode	Electrolytes	Output voltage [V]	Initial specific capacity [mAh g^{-1}]	Final specific capacity [mAh g^{-1}]	Cycles	Coulombic efficiency	Ref. No
Mo_6S_8	0.1 M $Mg[BH_4]_2$/1.5 M $LiBH_4$/DME	1.25	99.5	…	300	89.7%	[35]
Mo_6S_8	0.4 M APC/1.0 M LiCl/THF	1.2	105	98	3000	95%	[129]
Mo_6S_8	0.5 M OMBB*	1.2	-	80	1200	~100%	[130]
TiS_2	0.4 M APC/0.4 M LiCl/THF	1.5	158	150	400	~100%	[118]
$LiFePO_4$	0.4 M $MgCl_2$/0.4 M $AlCl_3$/1.0 M Li NTf_2/DME	2.6	130	90	100	~100%	[124]
MoS_2	0.4 M APC/1.0 M LiCl/THF	0.3	109	96.4	2300	~100%	[125]
$LiMn_2O_4$	0.5 M $Mg[NTf_2]_2$/0.5 M $LiNTf_2$/G2	2.8	106.0	53.8	50	~98%	[123]
$LiMn_2O_4$	0.25M $Mg[CB_{11}H_{12}]_2$/0.25M $LiNTf_2$/G4	…	80.6	59	30	~90%	[123]
TiO_2	0.5 M $Mg[BH_4]_2$/1.5 M $LiBH_4$/G4	0.8	…	126.3	6000	~100%	[111]
TiO_2	0.4 M APC/0.4 M LiCl/THF	0.8	110	212	200	~100%	[113]
FeS_2	0.2 M $Mg[BH_4]_2$/2.0 M $NaBH_4$/G2	1.0	228	160	40	~100%	[120]
V_2O_5	0.09 M $Mg[BH_4]_2$/0.25 M $NaBH_4$/G2	1.5	75	70	80	–	[121]
$FeFe(CN)_6$	0.4 M $MgCl_2$/0.4 M $AlCl_3$/0.4 M $NaAlCl_4$/DME	2.2	143	119	50	~98%	[131]
$Na_3V_2(PO_4)_3$	0.4 M $MgCl_2$/0.4 M $AlCl_3$/0.4 M $NaAlCl_4$/DME	2.6	104	85	50	~98%	[126]
$NaTi_2(PO_4)_3$	0.2 M $[Mg_2Cl_2]$ $[AlCl_4]_2$/ 0.4 M $NaAlCl_4$/DME	1.4	124	125	50	~98%	[132]

$$S_8 + 4e^- + 2Mg^{2+} \rightarrow 2MgS_4 \quad (1)$$

$$MgS_4 + 2e^- + Mg^{2+} \rightarrow 2MgS_2 \quad (2)$$

$$MgS_2 + 2e^- + Mg^{2+} \rightarrow 2MgS \quad (3)$$

The poor cyclability of the battery prototype could be due to the dissolution of the polysulfides generated upon discharging of the battery (which is also one of the main roadblocks in Li/S battery development).[133] Polysulfides are soluble to some extent in the polar electrolytes.[133,134,135] They can then be transported to the anode, creating a "shuttle" mechanism. This shuttle process causes loss of active material from the cathode, and reduces the performance in subsequent charge and discharge cycles. Thus, an electrolyte system in which polysulfides are less soluble, and remain in the vicinity of the cathode, is essential.

A range of Mg/S batteries, using different Mg electrolytes with different cations, anions, and solvents, have been studied to try to understand the chemistry within the electrolyte.[19,39–42,127,128,130] Some of these studies have resulted in significant improvements in the cyclability of the Mg/S battery. The carbon host material for the sulfur also significantly influences the charge-discharge cycling performance by trapping the polysulfides and thus weakening the shuttle effect in the solution.[20,22] ILs have been demonstrated to improve the electrolyte performance in Li/S batteries.[136] Mg/S battery studies also showed that adding ILs to the electrolytes can stabilize the polysulfide at the cathode side, improving cyclability.[127] Similar to Sulfur, Selenium (Se) can also be used as a conversion cathode material in Mg batteries. Theoretically, Se has a higher electronic conductivity and higher ionic conductivity during discharging compared to Sulfur. As a result Se can deliver faster kinetics and has a higher rate capability as a cathode material.[41,137,138] The cycling performance of Mg/S or Mg/Se batteries with different Mg electrolytes is summarized in Table 3.

3. Summary and Outlook

Although offering great potential as inexpensive and safe energy storage devices, rechargeable Mg batteries are still at the research stage. Current rechargeable Mg batteries remain far from comparable with lithium batteries in terms of cyclability, output voltage, and energy density. In particular, Mg electrolytes that are compatible with both a Mg anode and sufficiently high voltage cathodes do not yet deliver sufficient performance.

Although a range of Mg electrolytes have been demonstrated to support reversible Mg cycling over hundreds or

Table 3. Summary of performance of sulphur/Selenium cathodes with different Mg electrolytes.

S/Se cathode	Electrolytes	Output voltage [V]	Initial capacity [mAh g^{-1}]	Stable capacity [mAh g^{-1}]	Cycles	Ref. No
S-Carbon	0.5 M $AlCl_3$/1.5 M HMDSMgCl/THF	0.89	1200	…	2	[19]
S-CMK400PEG	1.8 M $AlCl_3$/0.9 M HMDSMgCl/G4/$PP_{14}TFSI$	1.6	800	260	20	[20]
S-CMK-3	0.3 M $AlCl_3$/0.6 M HMDSMgCl/C4mpyrTFSI/THF	0.7	~700	70	20	[127]
S-rGO	1.8 M $AlCl_3$/0.9 M HMDSMgCl/G4	~1.5	1028	219	50	[22]
S-CMK-3	0.6 M $Mg[B(hfp)_4]_2$/DME	~1.5	400	200	100	[39]
S-ACCS	0.4 M $Mg[B(hfp)_4]_2$/DME	~1.5	950	460	100	[139]
S-CNT	0.5 M $[Mg_4Cl_6(DME)_6][B(HFP)_4]_2$	~1.3	1200	1000	100	[130]
S-C	0.05 M MgF_2/0.5 M THFPB/DME	1.1	1081	825	30	[41]
S-C	0.05 M MgO/0.2 M THFPB/DME	1.1	520	1133	15	[40]
Se-C	0.05 M MgF_2/0.5 M THFPB/DME	0.8	420	600	10	[41]
Se-Cu	0.05 M MgF_2/0.5 M THFPB/DME	1.0	330	270	100	[138]

thousands of cycles, most of these systems contain corrosive species, such as chloride or Al^{3+} ions. Issues with currently studied non-corrosive electrolytes include the use of volatile organic solvents and poor reversibility. Impurities such H_2O are inevitable in Mg electrolytes, and thus electrolyte pre-treatment is often necessary; however, this still cannot guarantee high reversibility and low over-potential. This issue remains an obstacle in achieving a stable, long-lived metal electrode-electrolyte interface for RMBs. The design of new electrolytes may hold the promise of delivering high purity, thereby high compatibility with Mg anodes.

Furthermore, to obtain a high rate battery, a highly conductive electrolyte is essential. In addition to this, there is a dire need to move away from volatile and flammable electrolytes such as those based on ether solvents. Therefore, using ILs or mixtures of ILs with co-solvents to ensure a highly conductive and thermally stable electrolyte may overcome some of the current challenges.

Meanwhile, present cathode materials that can undergo stable charge-discharge for thousands of cycles are only able to deliver up to 1.5 V cell voltage, which limits energy density. As discussed, transition-metal oxide cathodes might be able to be used in RMBs with dual-salt (such as Mg/Li or Mg/Na) electrolytes. However, the metal deposited during charging needs to be carefully studied to avoid dendrite formation. Sulfur cathodes are compatible with some Mg electrolytes and can deliver a high energy capacity. Since reversible Mg deposition-stripping appears to be optimum in ether solvents, the issue of performance deterioration caused by dissolution of sulfur/polysulfide in these solvents must be addressed, especially when higher order glymes, such as tetraglyme, are used. Ionic liquids can improve the stability of the polysulfides formed on sulfur cathodes during discharge, and can minimize the "polysulfide shuttle" effect. Thus, such ionic liquids may enable a stable, high-capacity, rechargeable Mg/S battery.

Overall progress in the RMB is beginning to reveal pathways towards genuinely practical devices that can be competitive on cost while offering improved safety and sustainability. Nonetheless, there is tremendous scope for further optimisation of electrolytes and cathode materials, especially towards higher voltage cells.

Acknowledgements

The authors are grateful for the financial support from the Australian Research Council (ARC) through the ARC Centre of Excellence for Electromaterials Science (ACES). The authors would also like to acknowledge Dr Kate Nairn for proof reading and revising the manuscript.

Conflict of Interest

The authors declare no conflict of interest.

Keywords: cathodes · electrolytes · magnesium · magnesium batteries · rechargeable batteries

[1] H. Chen, T. N. Cong, W. Yang, C. Tan, Y. Li, Y. Ding, *Prog. Nat. Sci.* **2009**, *19*, 291–312.
[2] J. M. Tarascon, M. Armand, *Nature* **2001**, *414*, 359–367.
[3] D. Aurbach, Y. Gofer, A. Schechter, O. Chusid, H. Gizbar, Y. Cohen, M. Moshkovich, R. Turgeman, *J. Power Sources* **2001**, *97–8*, 269–273.
[4] N. Yoshimoto, M. Matsumoto, M. Egashia, M. Morita, *J. Power Sources* **2010**, *195*, 2096–2098.
[5] T. D. Gregory, R. J. Hoffman, R. C. Winterton, *J. Electrochem. Soc.* **1990**, *137*, 775–780.
[6] D. Aurbach, M. Moshkovich, A. Schechter, R. Turgeman, *Electrochem. Solid-State Lett.* **2000**, *3*, 31–34.
[7] D. Aurbach, Z. Lu, A. Schechter, Y. Gofer, H. Gizbar, R. Turgeman, Y. Cohen, M. Moshkovich, E. Levi, *Nature* **2000**, *407*, 724–727.
[8] D. Aurbach, H. Gizbar, A. Schechter, O. Chusid, H. E. Gottlieb, Y. Gofer, I. Goldberg, *J. Electrochem. Soc.* **2002**, *149*, A115–A121.
[9] H. Gizbar, Y. Vestfrid, O. Chusid, Y. Gofer, H. E. Gottlieb, V. Marks, D. Aurbach, *Organometallics* **2004**, *23*, 3826–3831.
[10] M. D. Levi, H. Gizbar, E. Lancry, Y. Gofer, E. Levi, D. Aurbach, *J. Electroanal. Chem.* **2004**, *569*, 211–223.
[11] M. D. Levi, E. Lancry, H. Gizbar, Z. Lu, E. Levi, Y. Gofer, D. Aurbach, *J. Electrochem. Soc.* **2004**, *151*, A1044–A1051.
[12] D. Aurbach, Y. Gofer, O. Chusid, E. Levi, M. D. Levi, Y. Vestfrid, H. Gizbar, E. Lancry, *Indian J. Chem. Sect. A* **2005**, *44*, 875–890.
[13] G. S. Suresh, M. D. Levi, D. Aurbach, *Electrochim. Acta* **2008**, *53*, 3889–3896.
[14] G. Gershinsky, H. D. Yoo, Y. Gofer, D. Aurbach, *Langmuir* **2013**, *29*, 10964–10972.
[15] C. J. Barile, R. Spatney, K. R. Zavadil, A. A. Gewirth, *J. Phys. Chem. C* **2014**, *118*, 10694–10699.
[16] H. D. Yoo, I. Shterenberg, Y. Gofer, G. Gershinsky, N. Pour, D. Aurbach, *Energy Environ. Sci.* **2013**, *6*, 2265–2279.
[17] O. Mizrahi, N. Amir, E. Pollak, O. Chusid, V. Marks, H. Gottlieb, L. Larush, E. Zinigrad, D. Aurbach, *J. Electrochem. Soc.* **2008**, *155*, A103–A109.
[18] Y. Cheng, T. Liu, Y. Shao, M. H. Engelhard, J. Liu, G. Li, *J. Mater. Chem. A* **2014**, *2*, 2473–2477.
[19] H. S. Kim, T. S. Arthur, G. D. Allred, J. Zajicek, J. G. Newman, A. E. Rodnyansky, A. G. Oliver, W. C. Boggess, J. Muldoon, *Nat. Commun.* **2011**, *2*.
[20] Z. Zhao-Karger, X. Zhao, D. Wang, T. Diemant, R. J. Behm, M. Fichtner, *Adv. Energy Mater.* **2015**, *5*.
[21] B. Pan, J. Huang, Z. Feng, L. Zeng, M. He, L. Zhang, J. T. Vaughey, M. J. Bedzyk, P. Fenter, Z. Zhang, A. K. Burrell, C. Liao, *Adv. Energy Mater.* **2016**, *6*, 1600140-n/a.
[22] B. Vinayan, Z. Zhao-Karger, T. Diemant, V. S. K. Chakravadhanula, N. I. Schwarzburger, M. A. Cambaz, R. J. Behm, C. Kübel, M. Fichtner, *Nanoscale* **2016**, *8*, 3296–3306.
[23] L. C. Merrill, J. L. Schaefer, *Langmuir* **2017**, *33*, 9426–9433.
[24] B. Pan, K.-C. Lau, J. T. Vaughey, L. Zhang, Z. Zhang, C. Liao, *J. Electrochem. Soc.* **2017**, *164*, A902–A906.
[25] J. T. Herb, C. A. Nist-Lund, C. B. Arnold, *ACS Energy Lett.* **2016**, *1*, 1227–1232.
[26] Y. Viestfrid, M. D. Levi, Y. Gofer, D. Aurbach, *J. Electroanal. Chem.* **2005**, *576*, 183–195.
[27] R. E. Doe, R. Han, J. Hwang, A. J. Gmitter, I. Shterenberg, H. D. Yoo, N. Pour, D. Aurbach, *Chem. Commun.* **2014**, *50*, 243–245.
[28] C. J. Barile, E. C. Barile, K. R. Zavadil, R. G. Nuzzo, A. A. Gewirth, *J. Phys. Chem. C* **2014**, *118*, 27623–27630.
[29] C. J. Barile, R. G. Nuzzo, A. A. Gewirth, *J. Phys. Chem. C* **2015**, *119*, 13524–13534.
[30] K. A. See, K. W. Chapman, L. Zhu, K. M. Wiaderek, O. J. Borkiewicz, C. J. Barile, P. J. Chupas, A. A. Gewirth, *J. Am. Chem. Soc.* **2016**, *138*, 328–337.
[31] K. See, Y.-M. Liu, Y. Ha, C. J. Barile, A. A. Gewirth, *ACS Appl. Mater. Interfaces* **2017**, *9*, 35729–35739.
[32] S. He, J. Luo, T. L. Liu, *J. Mater. Chem. A* **2017**, *5*, 12718–12722.
[33] F.-Y. Ma, in *Pitting Corrosion*, InTech, **2012**.
[34] R. Mohtadi, M. Matsui, T. S. Arthur, S.-J. Hwang, *Angew. Chem. Int. Ed.* **2012**, *51*, 9780–9783; *Angew. Chem.* **2012**, *124*, 9918–9921.
[35] Y. Y. Shao, T. B. Liu, G. S. Li, M. Gu, Z. M. Nie, M. Engelhard, J. Xiao, D. P. Lv, C. M. Wang, J. G. Zhang, J. Liu, *Sci. Rep.* **2013**, *3*, 3130.

[36] T. J. Carter, R. Mohtadi, T. S. Arthur, F. Mizuno, R. Zhang, S. Shirai, J. W. Kampf, *Angew. Chem. Int. Ed.* **2014**, *53*, 3173–3177; *Angew. Chem.* **2014**, *126*, 3237–3241.
[37] O. Tutusaus, R. Mohtadi, T. S. Arthur, F. Mizuno, E. G. Nelson, Y. V. Sevryugina, *Angew. Chem. Int. Ed.* **2015**, *54*, 7900–7904; *Angew. Chem.* **2015**, *127*, 8011–8015.
[38] O. Tutusaus, R. Mohtadi, N. Singh, T. S. Arthur, F. Mizuno, *ACS Energy Lett.* **2016**, *2*, 224–229.
[39] Z. Zhao-Karger, M. E. Gil Bardaji, O. Fuhr, M. Fichtner, *J. Mater. Chem. A* **2017**, *5*, 10815–10820.
[40] a) H. Xu, Z. Zhang, Z. Cui, A. Du, C. Lu, S. Dong, J. Ma, X. Zhou, G. Cui, *Electrochem. Commun.* **2017**, *83*, 72–76. b) A. Du, Z. Zhang, H. Qu, Z. Cui, L. Qiao, L. Wang, J. Chai, T. Lu, S. Dong, T. Dong, H. Xu, X. Zhou, G. Cui, *Energy Environ. Sci.* **2017**, *10*, 2616–2625.
[41] Z. Zhang, Z. Cui, L. Qiao, J. Guan, H. Xu, X. Wang, P. Hu, H. Du, S. Li, X. Zhou, S. Dong, Z. Liu, G. Cui, L. Chen, *Adv. Energy Mater.* **2017**, *7*, 1602055-n/a.
[42] Z. Zhao-Karger, R. Liu, W. Dai, Z. Li, T. Diemant, B. P. Vinayan, C. Bonatto Minella, X. Yu, A. Manthiram, R. J. Behm, M. Ruben, M. Fichtner, *ACS Energy Lett.* **2018**, *3*, 2005–2013.
[43] S. H. Lapidus, N. N. Rajput, X. Qu, K. W. Chapman, K. A. Persson, P. J. Chupas, *Phys. Chem. Chem. Phys.* **2014**, *16*, 21941–21945.
[44] I. Shterenberg, M. Salama, Y. Gofer, E. Levi, D. Aurbach, *MRS Bull.* **2014**, *39*, 453–460.
[45] L. Xue, D. D. DesMarteau, W. T. Pennington, *Solid State Sci.* **2005**, *7*, 311–318.
[46] S. Y. Ha, Y. W. Lee, S. W. Woo, B. Koo, J. S. Kim, J. Cho, K. T. Lee, N. S. Choi, *ACS Appl. Mater. Interfaces* **2014**, *6*, 4063–4073.
[47] G. Vardar, A. E. S. Sleightholme, J. Naruse, H. Hiramatsu, D. J. Siegel, C. W. Monroe, *ACS Appl. Mater. Interfaces* **2014**, *6*, 18033–18039.
[48] G. A. Giffin, J. Tannert, S. Jeong, W. Uhl, S. Passerini, *J. Phys. Chem. C* **2015**, *119*, 5878–5887.
[49] T. Kimura, K. Fujii, Y. Sato, M. Morita, N. Yoshimoto, *J. Phys. Chem. C* **2015**, *119*, 18911–18917.
[50] A. Kitada, Y. Kang, K. Matsumoto, K. Fukami, R. Hagiwara, K. Murase, *J. Electrochem. Soc.* **2015**, *162*, D389–D396.
[51] N. N. Rajput, X. Qu, N. Sa, A. K. Burrell, K. A. Persson, *J. Am. Chem. Soc.* **2015**, *137*, 3411–3420.
[52] T. Shiga, Y. Kato, M. Inoue, N. Takahashi, Y. Hase, *J. Phys. Chem. C* **2015**, *119*, 3488–3494.
[53] I. Shterenberg, M. Salama, H. D. Yoo, Y. Gofer, J.-B. Park, Y.-K. Sun, D. Aurbach, *J. Electrochem. Soc.* **2015**, *162*, A7118–A7128.
[54] A. Baskin, D. Prendergast, *J. Phys. Chem. C* **2016**, *120*, 3583–3594.
[55] J. G. Connell, B. Genorio, P. P. Lopes, D. Strmcnik, V. R. Stamenkovic, N. M. Markovic, *Chem. Mater.* **2016**, *28*, 8268–8277.
[56] M. M. Huie, C. A. Cama, P. F. Smith, J. Yin, A. C. Marschilok, K. J. Takeuchi, E. S. Takeuchi, *Electrochim. Acta* **2016**, *219*, 267–276.
[57] N. Sa, N. N. Rajput, H. Wang, B. Key, M. Ferrandon, V. Srinivasan, K. A. Persson, A. K. Burrell, J. T. Vaughey, *RSC Adv.* **2016**, *6*, 113663–113670.
[58] S. Terada, T. Mandai, S. Suzuki, S. Tsuzuki, K. Watanabe, Y. Kamei, K. Ueno, K. Dokko, M. Watanabe, *J. Phys. Chem. C* **2016**, *120*, 1353–1365.
[59] S. Hebié, H. P. K. Ngo, J.-C. Leprêtre, C. Iojoiu, L. Cointeaux, R. Berthelot, F. Alloin, *ACS Appl. Mater. Interfaces* **2017**, *9*, 28377–28385.
[60] Z. Ma, M. Kar, C. Xiao, M. Forsyth, D. R. MacFarlane, *Electrochem. Commun.* **2017**, *78*, 29–32.
[61] H. D. Yoo, S.-D. Han, I. L. Bolotin, G. M. Nolis, R. D. Bayliss, A. K. Burrell, J. T. Vaughey, J. Cabana, *Langmuir* **2017**, *33*, 9398–9406.
[62] M. Forsyth, P. C. Howlett, S. K. Tan, D. R. MacFarlane, N. Birbilis, *Electrochem. Solid-State Lett.* **2006**, *9*, B52–B55.
[63] P. C. Howlett, S. Zhang, D. R. MacFarlane, M. Forsyth, *Aust. J. Chem.* **2007**, *60*, 43–46.
[64] T. Ichitsubo, T. Adachi, S. Yagi, T. Doi, *J. Mater. Chem.* **2011**, *21*, 11764–11772.
[65] T. T. Tran, W. Lamanna, M. Obrovac, *J. Electrochem. Soc.* **2012**, *159*, A2005–A2009.
[66] M. Armand, F. Endres, D. R. MacFarlane, H. Ohno, B. Scrosati, *Nat. Mater.* **2009**, *8*, 621–629.
[67] S. Theivaprakasam, D. R. MacFarlane, S. Mitra, *Electrochim. Acta* **2015**, *180*, 737–745.
[68] G. A. Giffin, *J. Mater. Chem. A* **2016**, *4*, 13378–13389.
[69] M. Forsyth, G. M. A. Girard, A. Basile, M. Hilder, D. R. MacFarlane, F. Chen, P. C. Howlett, *Electrochim. Acta* **2016**, *220*, 609–617.
[70] M. Forsyth, H. Yoon, F. Chen, H. Zhu, D. R. MacFarlane, M. Armand, P. C. Howlett, *J. Phys. Chem. C* **2016**, *120*, 4276–4286.
[71] C. R. Pope, D. R. MacFarlane, M. Armand, M. Forsyth, L. A. O'Dell, *ChemPhysChem.* **2016**, *17*, 3187–3195.
[72] M. Kar, B. Winther-Jensen, M. Armand, T. J. Simons, O. Winther-Jensen, M. Forsyth, D. R. MacFarlane, *Electrochim. Acta* **2016**, *188*, 461–471.
[73] M. Kar, Z. Ma, L. M. Azofra, K. Chen, M. Forsyth, D. R. MacFarlane, *Chem. Commun.* **2016**, *52*, 4033–4036.
[74] Y. NuLi, J. Yang, R. Wu, *Electrochem. Commun.* **2005**, *7*, 1105–1110.
[75] G. T. Cheek, W. E. O'Grady, S. Z. El Abedin, E. M. Moustafa, F. Endres, *J. Electrochem. Soc.* **2008**, *155*, D91–D95.
[76] N. Amir, Y. Vestfrid, O. Chusid, Y. Gofer, D. Aurbach, *J. Power Sources* **2007**, *174*, 1234–1240.
[77] F. Bertasi, C. Hettige, F. Sepehr, X. Bogle, G. Pagot, K. Vezzu, E. Negro, S. J. Paddison, S. G. Greenbaum, M. Vittadello, V. Di Noto, *ChemSusChem* **2015**, *8*, 3069–3076.
[78] F. Bertasi, F. Sepher, G. Pagot, S. J. Paddison, V. Di Noto, *Adv. Funct. Mater.* **2016**.
[79] T. Watkins, A. Kumar, D. A. Buttry, *J. Am. Chem. Soc.* **2015**, *38*, 641–650.
[80] B. Lee, J.-H. Cho, H. R. Seo, S. B. Na, J. H. Kim, B. W. Cho, T. Yim, S. H. Oh, *J. Mater. Chem. A* **2018**, *6*, 3126–3133.
[81] Z. Ma, M. Forsyth, D. R. MacFarlane, M. Kar, *Green Energy Environ.* **2019**, doi.org/10.1016/j.gee.2018.10.003.
[82] S. Su, Y. NuLi, N. Wang, D. Yusipu, J. Yang, J. Wang, *J. Electrochem. Soc.* **2016**, *163*, D682–D688.
[83] M. Matsui, *J. Power Sources* **2011**, *196*, 7048–7055.
[84] S. Yagi, A. Tanaka, Y. Ichikawa, T. Ichitsubo, E. Matsubara, *Res. Chem. Intermed.* **2013**, *40*, 3–9.
[85] J. Luo, S. He, T. L. Liu, *ACS Energy Lett.* **2017**, *2*, 1197–1202.
[86] T. Yim, S.-G. Woo, S.-H. Lim, J.-Y. Yoo, W. Cho, M.-S. Park, Y.-K. Han, Y.-J. Kim, J. Yu, *ACS Sustainable Chem. Eng.* **2017**, *5*, 5733–5739.
[87] S. B. Son, T. Gao, S. P. Harvey, K. X. Steirer, A. Stokes, A. Norman, C. S. Wang, A. Cresce, K. Xu, C. M. Ban, *Nat. Chem.* **2018**, *10*, 532–539.
[88] Y. Liang, R. Feng, S. Yang, H. Ma, J. Liang, J. Chen, *Adv. Mater.* **2011**, *23*, 640–643.
[89] C. Ling, D. Banerjee, M. Matsui, *Electrochim. Acta* **2012**, *76*, 270–274.
[90] D. J. Wetzel, M. A. Malone, R. T. Haasch, Y. Meng, H. Vieker, N. T. Hahn, A. Gölzhäuser, J.-M. Zuo, K. R. Zavadil, A. A. Gewirth, R. G. Nuzzo, *ACS Appl. Mater. Interfaces* **2015**, *7*, 18406–18414.
[91] D. J. Wetzel, M. A. Malone, A. A. Gewirth, R. G. Nuzzo, *Electrochim. Acta* **2017**, *229*, 112–120.
[92] W. Kaveevivitchai, A. J. Jacobson, *Chem. Mater.* **2016**, *28*, 4593–4601.
[93] E. Levi, M. D. Levi, O. Chasid, D. Aurbach, *J. Electroceram.* **2009**, *22*, 13–19.
[94] E. Levi, Y. Gofer, D. Aurbach, *Chem. Mater.* **2010**, *22*, 860–868.
[95] R. Zhang, C. Ling, *MRS Energy Sustainability#j.hofmann – 16.08.2017 11:12:13* **2016**, *3*.
[96] P. Saha, M. K. Datta, O. I. Velikokhatnyi, A. Manivannan, D. Alman, P. N. Kumta, *Prog. Mater. Sci.* **2014**, *66*, 1–86.
[97] C. B. Bucur, T. Gregory, A. G. Oliver, J. Muldoon, *J. Phys. Chem. Lett.* **2015**, *6*, 3578–3591.
[98] O. Tutusaus, R. Mohtadi, *ChemElectroChem* **2015**, *2*, 51–57.
[99] P. Canepa, G. Sai Gautam, D. C. Hannah, R. Malik, M. Liu, K. G. Gallagher, K. A. Persson, G. Ceder, *Chem. Rev.* **2017**, *117*, 4287–4341.
[100] F. Tuerxun, Y. Abulizi, Y. N. NuLi, S. J. Su, J. Yang, J. L. Wang, *J. Power Sources* **2015**, *276*, 255–261.
[101] A. J. Crowe, K. K. Stringham, B. M. Bartlett, *ACS Appl. Mater. Interfaces* **2016**, *8*, 23060–23065.
[102] J. T. Herb, C. A. Nist-Lund, C. B. Arnold, *J. Mater. Chem. A* **2017**, *5*, 7801–7805.
[103] S.-J. Kang, S.-C. Lim, H. Kim, J. W. Heo, S. Hwang, M. Jang, D. Yang, S.-T. Hong, H. Lee, *Chem. Mater.* **2017**, *29*, 3174–3180.
[104] D. Imamura, M. Miyayama, *Solid State Ionics* **2003**, *161*, 173–180.
[105] Q. An, Y. Li, H. Deog Yoo, S. Chen, Q. Ru, L. Mai, Y. Yao, *Nano Energy* **2015**, *18*, 265–272.
[106] S. Rasul, S. Suzuki, S. Yamaguchi, M. Miyayama, *Electrochim. Acta* **2012**, *82*, 243–249.
[107] R. Zhang, X. Yu, K.-W. Nam, C. Ling, T. S. Arthur, W. Song, A. M. Knapp, S. N. Ehrlich, X.-Q. Yang, M. Matsui, *Electrochem. Commun.* **2012**, *23*, 110–113.
[108] C. Yuan, Y. Zhang, Y. Pan, X. Liu, G. Wang, D. Cao, *Electrochim. Acta* **2014**, *116*, 404–412.
[109] J.-S. Kim, W.-S. Chang, R.-H. Kim, D.-Y. Kim, D.-W. Han, K.-H. Lee, S.-S. Lee, S.-G. Doo, *J. Power Sources* **2015**, *273*, 210–215.
[110] R. Zhang, T. S. Arthur, C. Ling, F. Mizuno, *J. Power Sources* **2015**, *282*, 630–638.

[111] S. Su, Y. NuLi, Z. Huang, Q. Miao, J. Yang, J. Wang, *ACS Appl. Mater. Interfaces* **2016**, *8*, 7111–7117.
[112] M. Zhang, A. C. MacRae, H. Liu, Y. S. Meng, *J. Electrochem. Soc.* **2016**, *163*, A2368–A2370.
[113] Y. Meng, D. S. Wang, Y. J. Wei, K. Zhu, Y. Y. Zhao, X. F. Bian, F. Du, B. B. Liu, Y. Gao, G. Chen, *J. Power Sources* **2017**, *346*, 134–142.
[114] L. Zhou, Q. Liu, Z. Zhang, K. Zhang, F. Xiong, S. Tan, Q. An, Y.-M. Kang, Z. Zhou, L. Mai, *Adv. Mater.* **2018**, *30*, 1801984.
[115] J. Song, E. Sahadeo, M. Noked, S. B. Lee, *J. Phys. Chem. Lett.* **2016**, *7*, 1736–1749.
[116] G. S. Gautam, P. Canepa, W. D. Richards, R. Malik, G. Ceder, *Nano Lett.* **2016**, *16*, 2426–2431.
[117] J. Yin, A. B. Brady, E. S. Takeuchi, A. C. Marschilok, K. J. Takeuchi, *Chem. Commun.* **2017**.
[118] T. Gao, F. D. Han, Y. J. Zhu, L. M. Suo, C. Luo, K. Xu, C. S. Wang, *Adv. Energy Mater.* **2015**, *5*.
[119] T. Ichitsubo, S. Okamoto, T. Kawaguchi, Y. Kumagai, F. Oba, S. Yagi, N. Goto, T. Doi, E. Matsubara, *J. Mater. Chem. A* **2015**, *3*, 10188–10194.
[120] M. Walter, K. V. Kravchyk, M. Ibáñez, M. V. Kovalenko, *Chem. Mater.* **2015**, *27*, 7452–7458.
[121] M. Cabello, F. Nacimiento, R. Alcántara, P. Lavela, G. Ortiz, J. L. Tirado, *J. Electrochem. Soc.* **2016**, *163*, A2781–A2790.
[122] Y. Cheng, H. J. Chang, H. Dong, D. Choi, V. L. Sprenkle, J. Liu, Y. Yao, G. Li, *J. Mater. Res.* **2016**, *31*, 3125–3141.
[123] B. Pan, Z. Feng, N. Sa, S.-D. Han, Q. Ma, P. Fenter, J. T. Vaughey, Z. Zhang, C. Liao, *Chem. Commun.* **2016**, *52*, 9961–9964.
[124] Y. W. Cheng, D. W. Choi, K. S. Han, K. T. Mueller, J. G. Zhang, V. L. Sprenkle, J. Liu, G. S. Li, *Chem. Commun.* **2016**, *52*, 5379–5382.
[125] Y. Ju, Y. Meng, Y. Wei, X. Bian, Q. Pang, Y. Gao, F. Du, B. Liu, G. Chen, *Chem. Eur. J.* **2016**, *22*, 18073–18079.
[126] Y. Li, Q. An, Y. Cheng, Y. Liang, Y. Ren, C.-J. Sun, H. Dong, Z. Tang, G. Li, Y. Yao, *Nano Energy* **2017**, *34*, 188–194.
[127] W. Li, S. Cheng, J. Wang, Y. Qiu, Z. Zheng, H. Lin, S. Nanda, Q. Ma, Y. Xu, F. Ye, M. Liu, L. Zhou, Y. Zhang, *Angew. Chem. Int. Ed.* **2016**, *128*, 6516–6520.
[128] G. Bieker, J. Wellmann, M. Kolek, K. Jalkanen, M. Winter, P. Bieker, *Phys. Chem. Chem. Phys.* **2017**, *19*, 11152–11162.
[129] Y. Cheng, Y. Shao, J.-G. Zhang, V. L. Sprenkle, J. Liu, G. Li, *Chem. Commun.* **2014**, *50*, 9644–9646.
[130] A. Du, Z. Zhang, H. Qu, Z. Cui, L. Qiao, L. Wang, J. Chai, T. Lu, S. Dong, T. Dong, H. Xu, X. Zhou, G. Cui, *Energy Environ. Sci.* **2017**, *10*, 2616–2625.
[131] H. Dong, Y. Li, Y. Liang, G. Li, C.-J. Sun, Y. Ren, Y. Lu, Y. Yao, *Chem. Commun.* **2016**, *52*, 8263–8266.
[132] Y. Xu, W. Cao, Y. Yin, J. Sheng, Q. An, Q. Wei, W. Yang, L. Mai, *Nano Energy* **2019**, *55*, 526–533.
[133] Y. V. Mikhaylik, J. R. Akridge, *J. Electrochem. Soc.* **2004**, *151*, A1969–A1976.
[134] T. Gao, X. Ji, S. Hou, X. Fan, X. Li, C. Yang, F. Han, F. Wang, J. Jiang, K. Xu, C. Wang, *Adv. Mater.* **2017**, 1704313-n/a.
[135] X. Zhou, J. Tian, J. Hu, C. Li, *Adv. Mater.* **2018**, *30*, 1704166-n/a.
[136] J.-W. Park, K. Ueno, N. Tachikawa, K. Dokko, M. Watanabe, *J. Phys. Chem. C* **2013**, *117*, 20531–20541.
[137] C.-P. Yang, Y.-X. Yin, Y.-G. Guo, *J. Phys. Chem. Lett.* **2015**, *6*, 256–266.
[138] Z. Zhang, B. Chen, H. Xu, Z. Cui, S. Dong, A. Du, J. Ma, Q. Wang, X. Zhou, G. Cui, *Adv. Funct. Mater.* **2018**, *28*, 1701718.
[139] Z. Zhao-Karger, R. Liu, W. Dai, Z. Li, T. Diemant, B. P. Vinayan, C. Bonatto Minella, X. Yu, A. Manthiram, R. J. Behm, M. Ruben, M. Fichtner, *ACS Energy Lett.* **2018**.

Manuscript received: October 11, 2018
Revised manuscript received: December 14, 2018
Version of record online: January 28, 2019